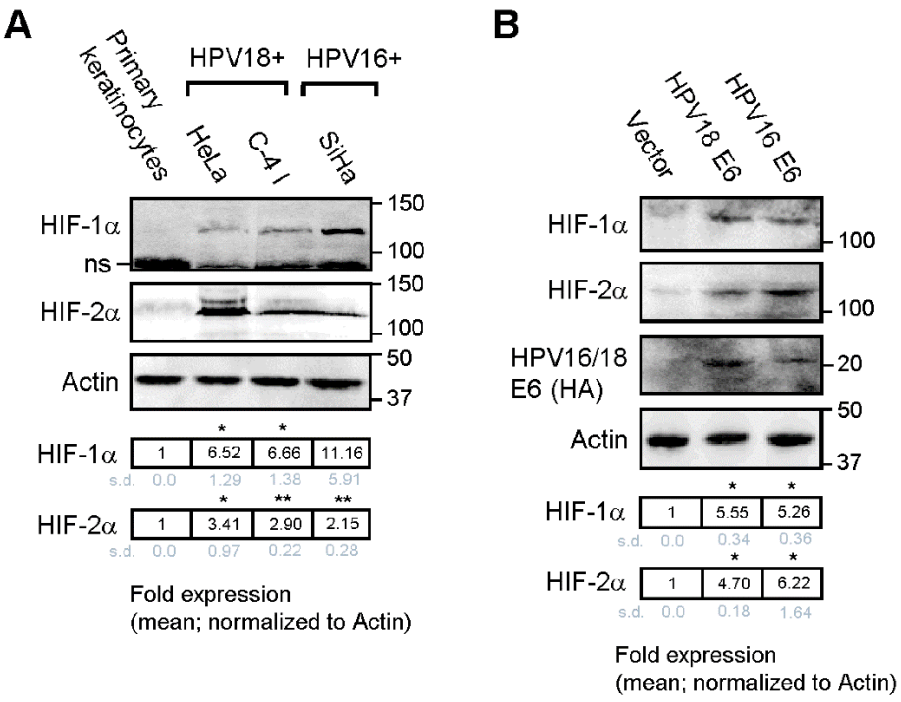

Supplemental Fig. S1. Human papillomavirus-transformed cervical carcinoma cell-lines and E6-expressing transfected cells contain increased levels of HIF-1α and HIF-2α. (A) The hypoxic markers HIF-1α and HIF-2α were detected in HPV18+ (HeLa and C-4 I) and HPV16+ (SiHa) cervical carcinoma cell-lines by immunoblotting with densitometric quantification. (B) HT-1080 cells were transfected with expression constructs for HPV18 or HPV16 E6 (HA-tagged), or an empty CβS vector as negative control and the expression of HIF-1α, HIF-2α, and the viral E6 (HA) oncoprotein was detected by immunoblotting. Actin is shown as a protein loading control. N-value = 3. The asterisks denote statistical significance as determined using Student's t-test (*$P < 0.0332$, **$P < 0.0021$).

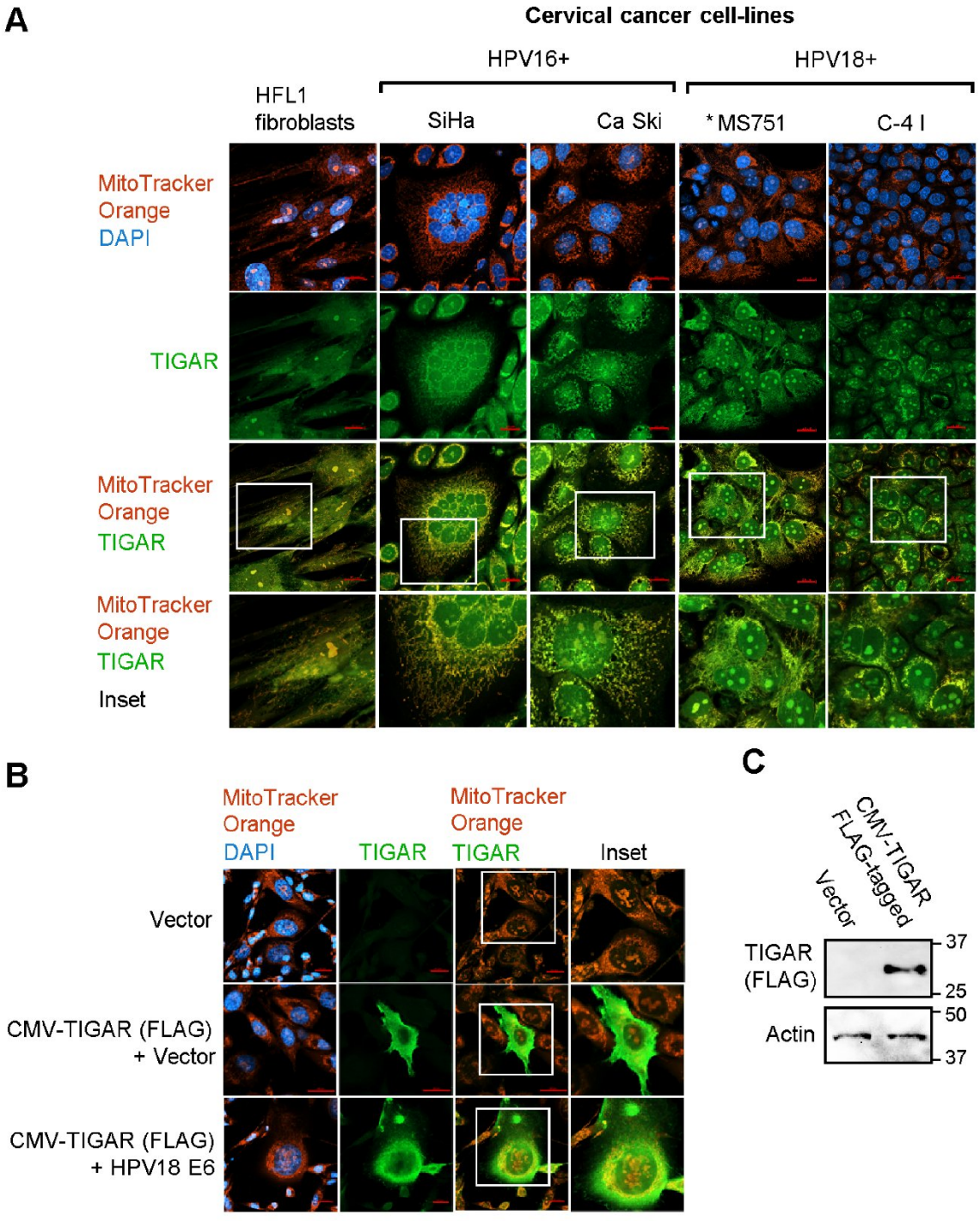

Supplemental Fig. S2. Hypoxia-independent mitochondrial targeting of the TIGAR protein in hrHPV-transformed cervical carcinoma cells. (A) Mitochondrial localization of the TIGAR protein in HPV16-transformed (SiHa and Ca Ski) and HPV18-transformed (MS751 and C-4 I) cervical carcinoma cell-lines was visualized by labeling the samples with MitoTracker Orange (red signal) and then performing immunofluorescence-confocal microscopy using an Anti-TIGAR primary antibody (green signal; *the MS751 cell-line also contains HPV45 sequences). Immortalized human HFL1 fibroblasts (HPV-negative) are shown for comparison and exhibited reduced, broadly diffuse TIGAR expression. DAPI nuclear-

staining (blue signal) is provided for reference in the merged images. Scale bar, 20 µm. The enlarged inset areas (bottom panels) depict colocalization between TIGAR and the MitoTracker Orange probe in hrHPV-transformed cells. (B) The hypoxia-independent mitochondrial targeting of TIGAR in transfected cells expressing the HPV18 E6 oncoprotein was further verified by cotransfecting the cells with CMV-TIGAR (FLAG-tagged) and labeling the cells with MitoTracker Orange, followed by immunofluorescence-confocal imaging analysis. Scale bar, 20 µm. The TIGAR (FLAG) protein in cells containing HPV18 E6 notably exhibited punctate colocalization with the MitoTracker Orange probe (see inset). (C) The expression of the FLAG-tagged TIGAR protein was detected by immunoblotting extracts from HPV18+ HeLa cells transfected with CMV-TIGAR (FLAG). An empty CβS vector was included as a negative control. Actin is shown as a protein loading control. N-value = 3.

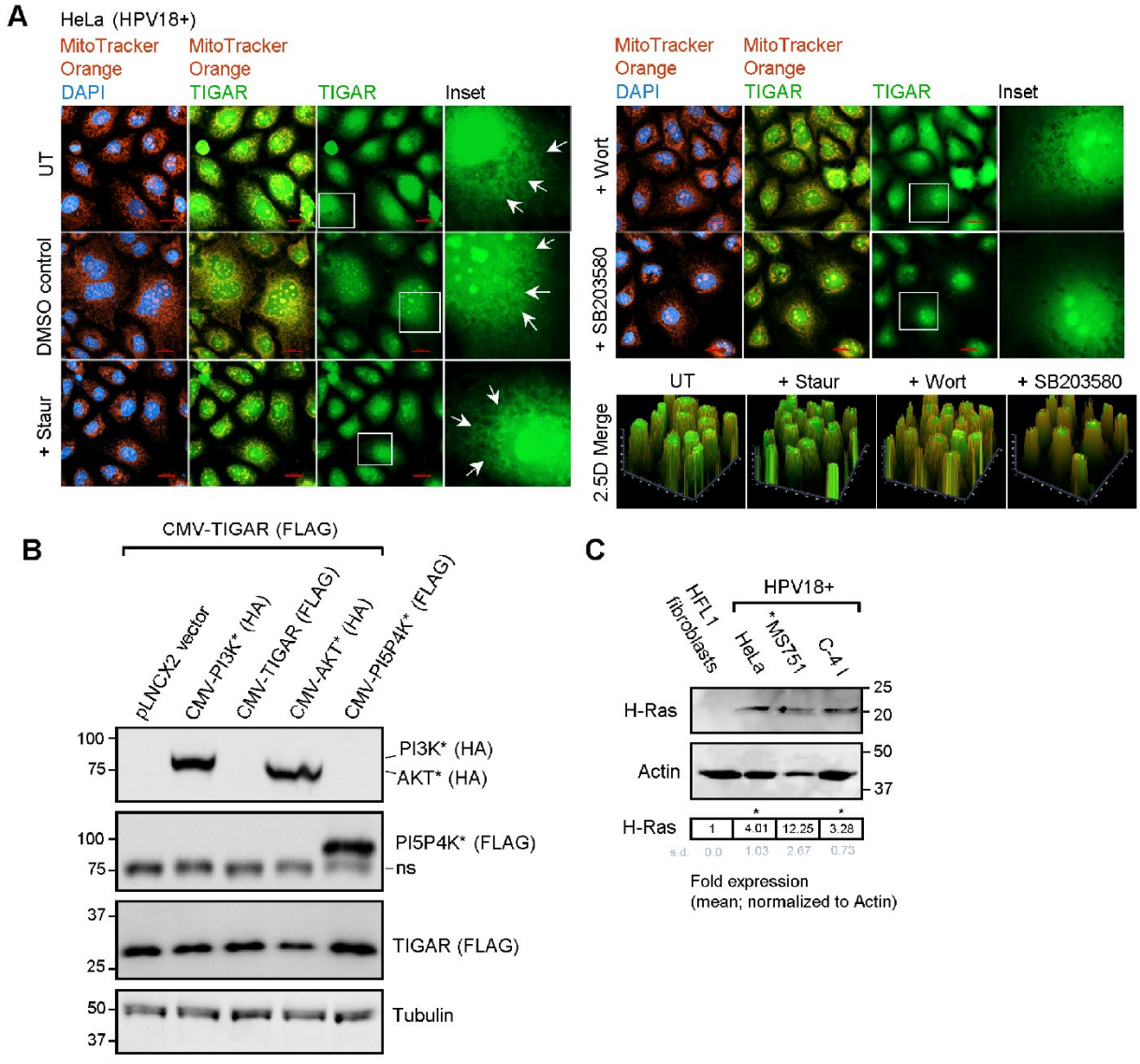

Supplemental Fig. S3. The hrHPV E6-induced mitochondrial targeting of TIGAR requires the activation of cellular kinases. (A) HPV18-transformed HeLa cervical carcinoma cells were treated with various chemical kinase inhibitors (i.e., staurosporine, wortmannin, or SB203580; Millipore-Sigma) or a DMSO solvent control and then the cells were labeled with MitoTracker Orange (red signal) and immunofluorescence-confocal microscopy was performed using an Anti-TIGAR primary antibody (green signal) to visualize mitochondrial targeting of the TIGAR protein. UT, untreated cells. DAPI nuclear-

staining (blue signal) is provided for reference. Scale bar, 20 μm. The enlarged inset areas show the subcellular distribution of the TIGAR protein. The inhibitors, wortmannin (inhibits PI3K-related kinases) and SB203580 (inhibits p38MAPK), but neither staurosporine nor the DMSO solvent control, markedly blocked the localization of TIGAR to mitochondrial membranes (see arrows) consistent with their ability to inhibit serine-phosphorylation of the TIGAR protein as shown in Fig. 2B. The relative fluorescence-intensities and overlap between the TIGAR and MitoTracker Orange signals are graphically represented in the 2.5D Merged images (lower right panels). (B) The expression of the constitutively-active mutants of PI3K (HA), PI5P4K (FLAG), and AKT (HA) as well as the TIGAR (FLAG-tagged) protein used in Fig. 2C was detected by immunoblotting. "ns" denotes a nonspecific band. (C) The involvement of PI3K/PI5P4K and MAPK in the E6-induced mitochondrial targeting of TIGAR suggests that Ras-signaling could activate these Ras effector-loop binding factors. Indeed, the HPV18+ cervical carcinoma cell-lines, HeLa, MS751, and C-4 I, were found to contain elevated levels of H-Ras as compared to (HPV-negative) HFL1 fibroblasts. The H-Ras protein was detected by immunoblotting and quantified by densitometry. N-value = 3. The asterisks denote statistical significance as determined using Student's t-test (*$P < 0.0332$).

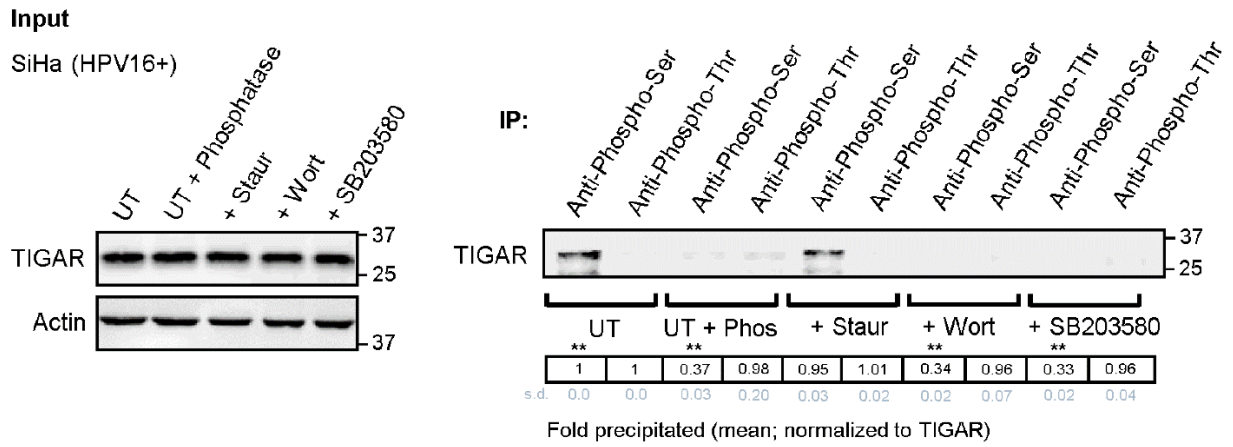

Supplemental Fig. S4. The HPV16+ cervical cancer cell-line, SiHa, exhibits hypoxia-independent phosphorylation of the TIGAR protein that is inhibited by the chemical kinase-inhibitors wortmannin and SB203580, but not staurosporine. SiHa cells were treated with various chemical kinase inhibitors as described and then immunoprecipitations were performed using phospho-specific monoclonal antibodies (Anti-Phospho-Serine and Anti-Phospho-Threonine) and Protein-G agarose. As a control for the phospho-specific antibodies, the SiHa cell extract was treated for 1 hr at 37°C with a recombinant Serine/threonine-protein phosphatase (2,000 U; Abcam) prior to immunoprecipitation (UT + Phos lanes). The input levels of TIGAR and Actin were detected by immunoblotting and are shown in the left panels. The immunoprecipitated phosphorylated TIGAR protein was detected by immunoblotting and quantified by densitometry (right panels). N-value = 3. The asterisks denote statistical significance as determined using Student's t-test (*$P < 0.0332$, **$P < 0.0021$).

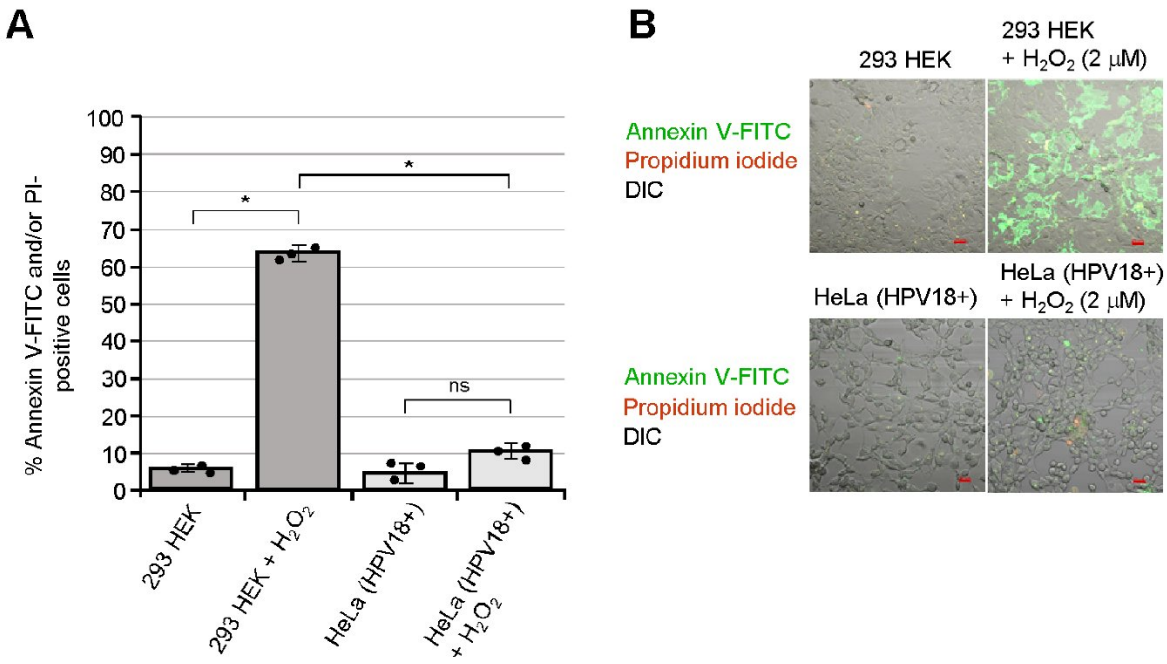

Supplemental Fig. S5. Human papillomavirus-transformed cells are generally more resistant to oxidative stress-induced cytotoxicity than HPV-negative cells. (A and B). 293 HEK (HPV-neg) cells and HPV18+ HeLa cells were treated with hydrogen peroxide (H_2O_2; 2 μM) for 2 hrs and then the samples were stained with Annexin V-FITC and PI and the relative percentages of apoptotic cells were quantified by confocal microscopy and counting at 20x magnification. A DIC filter was included in the merged images to visualize all the cells (in B). Scale bar, 20 μm. N-value = 3. The asterisks denote statistical significance as determined using unpaired two-tailed Student's t-tests (*$P < 0.0332$).

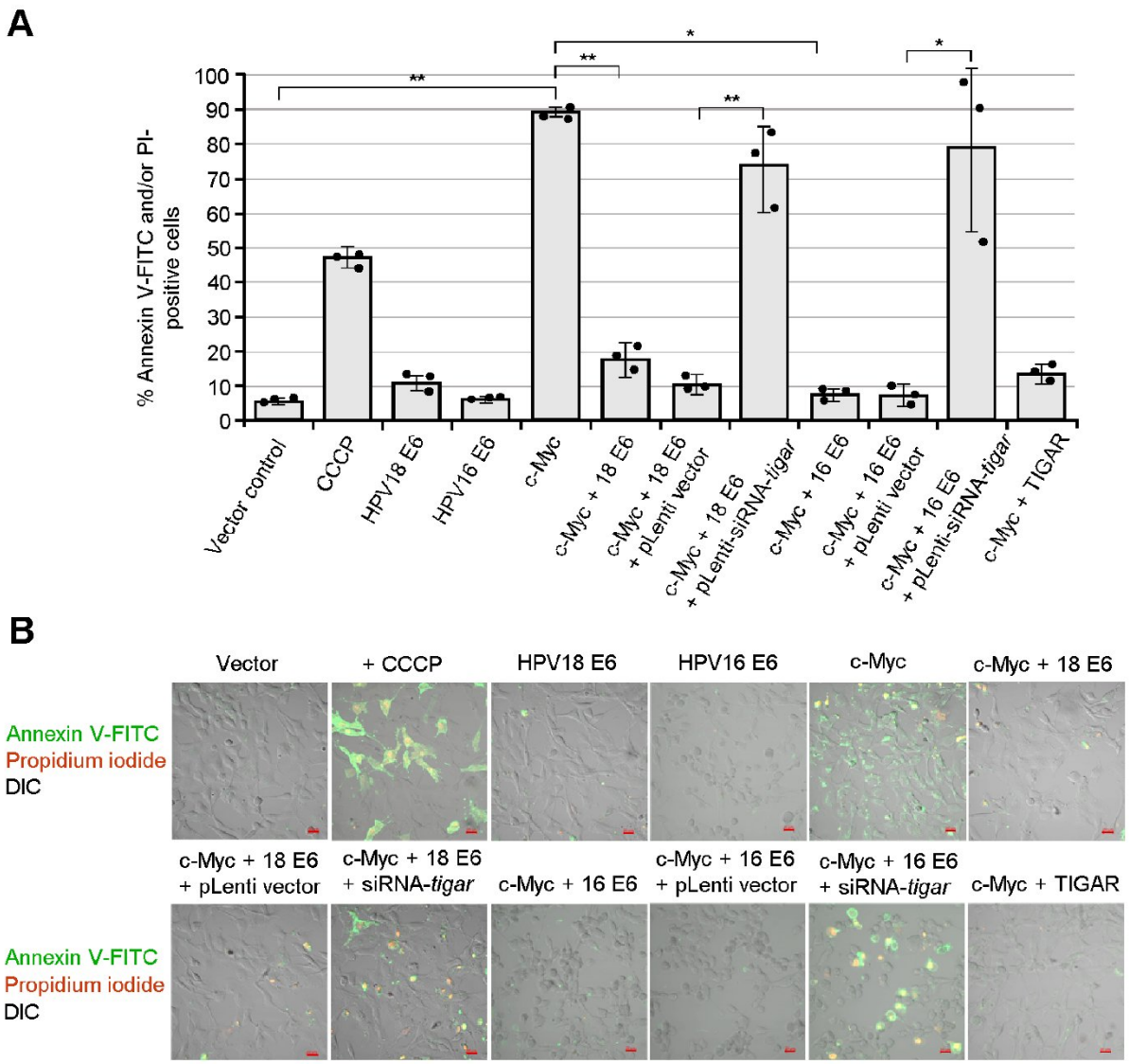

Supplemental Fig. S6. High-risk HPV E6 oncoproteins prevent c-Myc-induced apoptosis in a TIGAR-dependent manner. (A and B) The ability of the viral E6 oncoprotein to prevent c-Myc-induced cellular apoptosis was evaluated by cotransfecting HT-1080 cells with CβF-c-Myc and expression constructs for HPV18 E6 or HPV16 E6. Certain samples were also transduced with lentiviral-siRNA-*tigar* to inhibit endogenous TIGAR expression or an empty pLenti vector as negative control. The cells were cotransfected with CβF-c-Myc and CMV-TIGAR for comparison. As a positive apoptosis control, one sample was treated with CCCP (50 μM). The cells were then stained with Annexin V-FITC (green signal) and PI (red signal) and confocal microscopy was performed to quantify the relative percentages of apoptotic cells (Annexin V-FITC and/or PI-positive cells) per field by counting triplicate visual fields at 200x magnification (n-value = 3). Error bars represent mean ± SD. N-value = 3. Scale bar, 20 μm. The asterisks denote statistical significance as determined using unpaired two-tailed Student's t-tests (*$P < 0.0332$, **$P < 0.0021$).

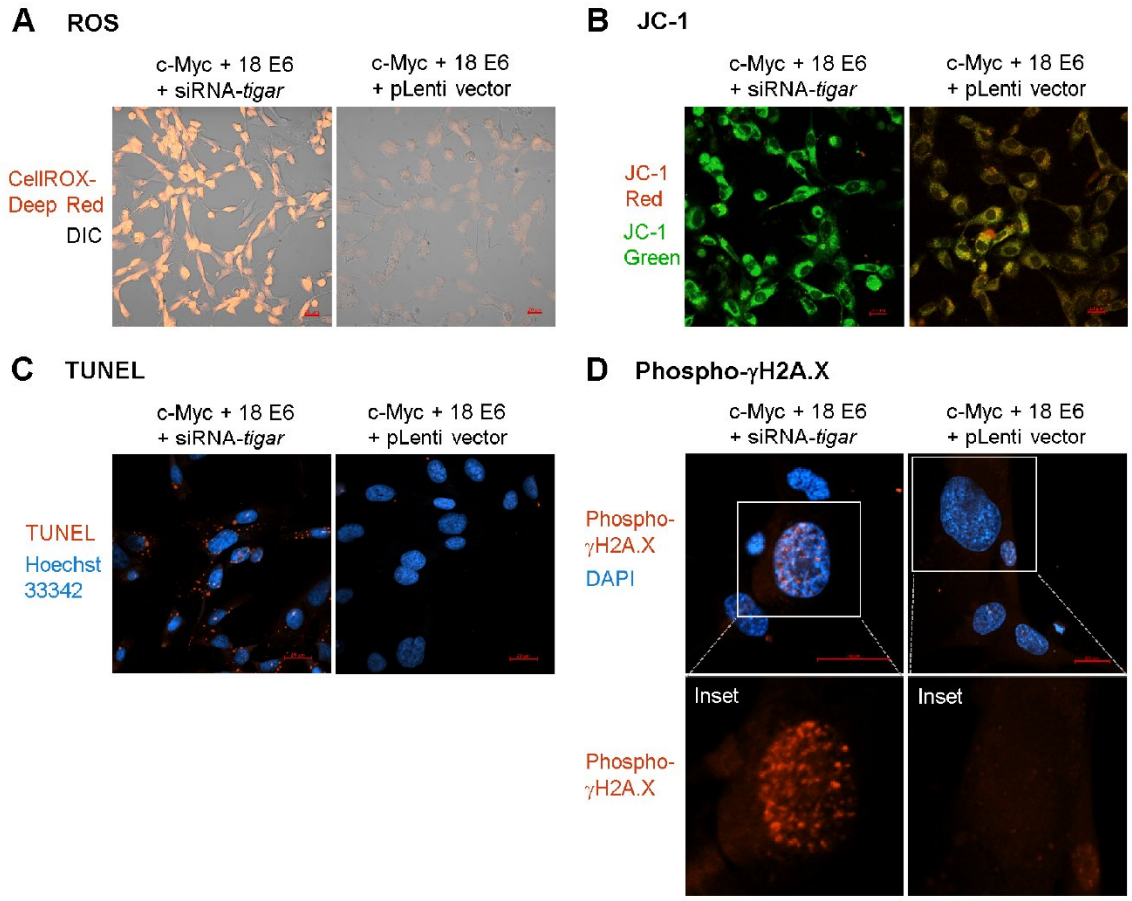

Supplemental Fig. S7. The ability of the HPV18 E6 oncoprotein to protect against c-Myc-induced oxidative damage and genotoxicity is dependent upon TIGAR functions. (A) Intracellular ROS were detected using the fluorescent probe, CellROX-Deep Red, and the cells were visualized by confocal microscopy with the inclusion of a DIC filter in merged images. Representative micrographs are shown for HT-1080 cells that were cotransfected with CβF-c-Myc and an expression construct for HPV18 E6 and then transduced with either lentiviral-siRNA-*tigar* or an empty pLenti vector as negative control. The data were quantified and graphically depicted in Fig. 3B. (B) Mitochondrial damage/membrane depolarization (green signal) and normal polarized mt membranes (red signal) were visualized in cells expressing HPV18 E6/c-Myc and lentiviral-siRNA-*tigar* or an empty pLenti vector by staining the cells with the fluorescent JC-1 probe for analysis by confocal microscopy. Representative merged images are shown. The quantified data is graphically presented in Fig. 3C. (C) Oxidative DNA-damage was visualized in cotransfected cells expressing HPV18 E6/c-Myc and either lentiviral-siRNA-*tigar* or an empty pLenti vector by staining the cells using a 594 nm fluorescent Click-iT Plus TUNEL kit (Invitrogen) and then performing confocal microscopy. Hoechst 33342 nuclear-staining is provided in the merged images. The quantified data is shown in Fig. 4A. (D) Incorporation of the phosphorylated histone variant, γH2A.X, at sites of damaged chromatin (red foci) in cells expressing HPV18E6/c-Myc and lentiviral-siRNA-*tigar* or an empty pLenti vector was visualized by immunofluorescence-confocal microscopy. DAPI nuclear-staining is provided for reference in the merged images. Enlarged inset areas are shown in the lower panels. The data was quantified and is graphically presented in Fig. 4B. Scale bars, 20 μm. N-value = 3.

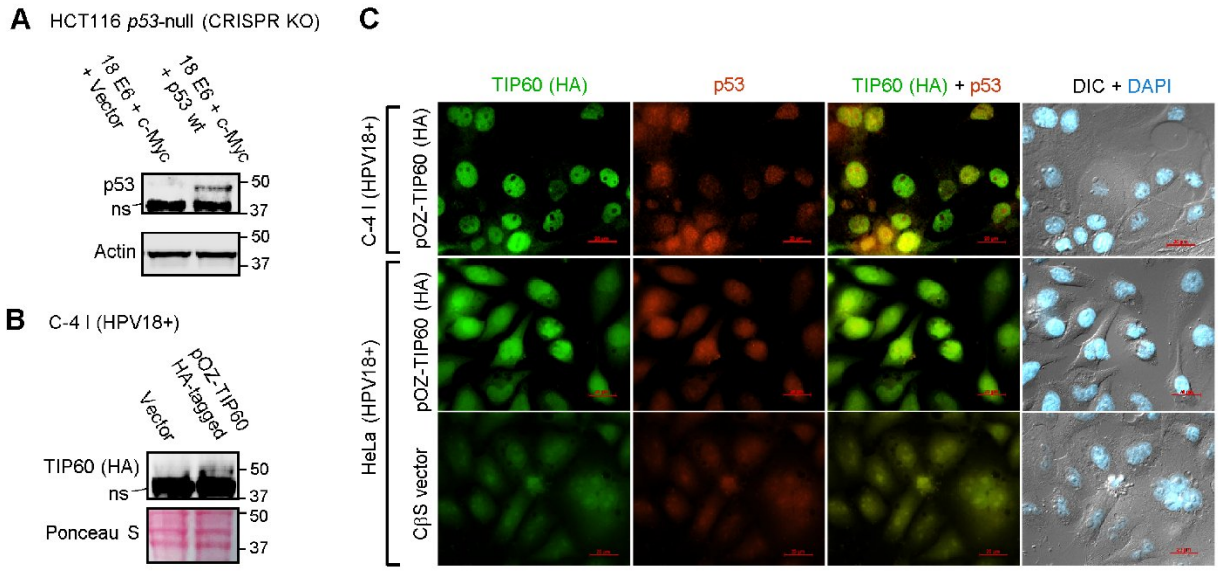

Supplemental Fig. S8. Expression of the p53 and TIP60 proteins in transfected cells. (A) The p53 protein in HCT116 *p53*$^{-/-}$ (homozygous *p53* CRISPR KO) carcinoma cells that were transfected with expression constructs for HPV18 E6, c-Myc, and either wild-type p53 or an empty CβS vector control, as shown in Figs. 5C and 5D, was detected by immunoblotting. (B) The ectopically expressed TIP60 (HA) protein was detected in transfected HPV18+ C-4 I cervical carcinoma cells by immunoblotting using a rabbit polyclonal Anti-HA (Y-11) primary antibody. "ns" denotes nonspecific bands. (C) The HPV18-transformed cervical carcinoma cell-lines, HeLa and C-4 I, were transfected with a pOZ-TIP60 (HA-tagged) expression construct or an empty CβS vector as shown in Figs. 5A and 5B, and the HA-tagged TIP60 (green signal) and p53 (red signal) proteins were detected by immunofluorescence-microscopy. DAPI nuclear-staining (blue signal) and DIC phase-contrast merged images are provided for reference. Scale bar, 20 μm. N-value = 3.

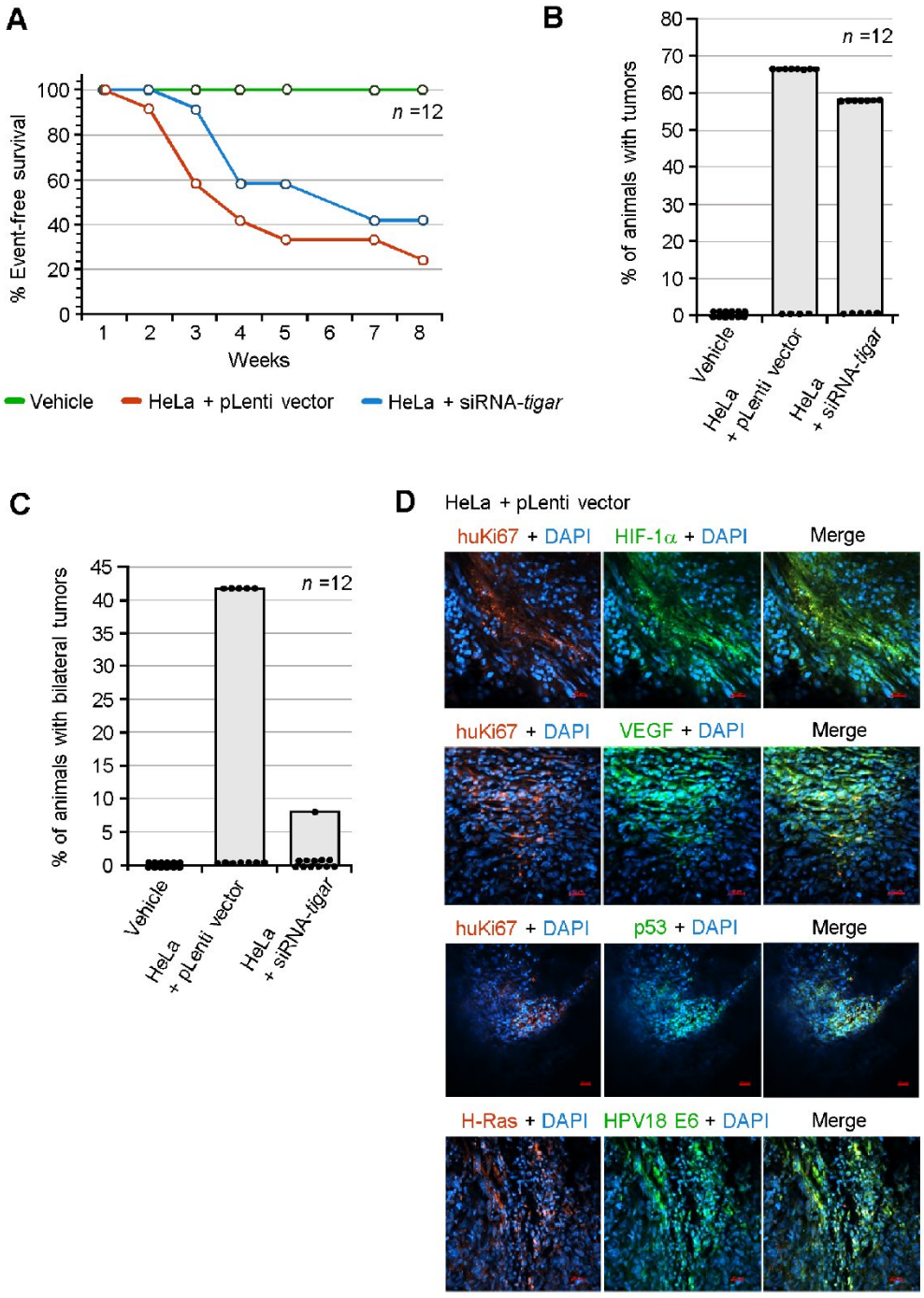

Supplemental Fig. S9. The siRNA-inhibition of TIGAR expression inhibits in vivo tumorigenesis in a xenograft model of hrHPV-induced carcinoma. (A) To determine if TIGAR functions are required for HPV-induced tumor formation and disease progression in vivo, athymic NIH III-nude mice were subcutaneously engrafted over each hind flank with HPV18+ HeLa adenocarcinoma cells that had been transduced with either lentiviral-siRNA-*tigar* or an empty lentiviral (pLenti) vector as a negative control. Another group of animals was injected with the Vehicle alone for comparison (n-value = 12). The experimental animals were closely monitored over a period of 8 weeks for the development and growth of primary tumors at the injection sites. A Kaplan-Meier plot of event-free survival demonstrates that the HeLa/siRNA-*tigar* engrafted animals exhibited delayed tumor formation as compared to the HeLa/pLenti vector sample group.

(B and C) Although a similar number of animals (58% versus 66%) developed tumors in both the HeLa/siRNA-*tigar* and HeLa/pLenti vector experimental groups (in B), fewer HeLa/siRNA-*tigar* engrafted animals exhibited bilateral tumor-growth as compared to the HeLa/pLenti vector group (in C). (D) The HPV18+ HeLa/pLenti vector xenograft tumors express H-Ras, p53, and the angiogenic markers, HIF-1α and VEGF. The primary tumor masses were harvested from experimental NIH III-nude animals that were engrafted with HPV18+ HeLa cells transduced with the empty pLenti vector (n-value = 12) and then fixed and immunostained using Anti-human Ki67 (huKi67), Anti-HIF-1α, Anti-VEGF, Anti-H-Ras, Anti-p53, and Anti-HPV18 E6 primary antibodies. DAPI nuclear-staining is included for reference in the merged images. Immunofluorescence-confocal microscopy was performed to visualize the expression of HIF-1α, VEGF, and p53 (green signals) in the huKi67-positive (red signal) engrafted HeLa tumor cells, as well as H-Ras expression (red signal) in the HPV18 E6-positive (green signal) HeLa tumor cells. The data shown is representative of triplicate sections analyzed for each primary tumor.

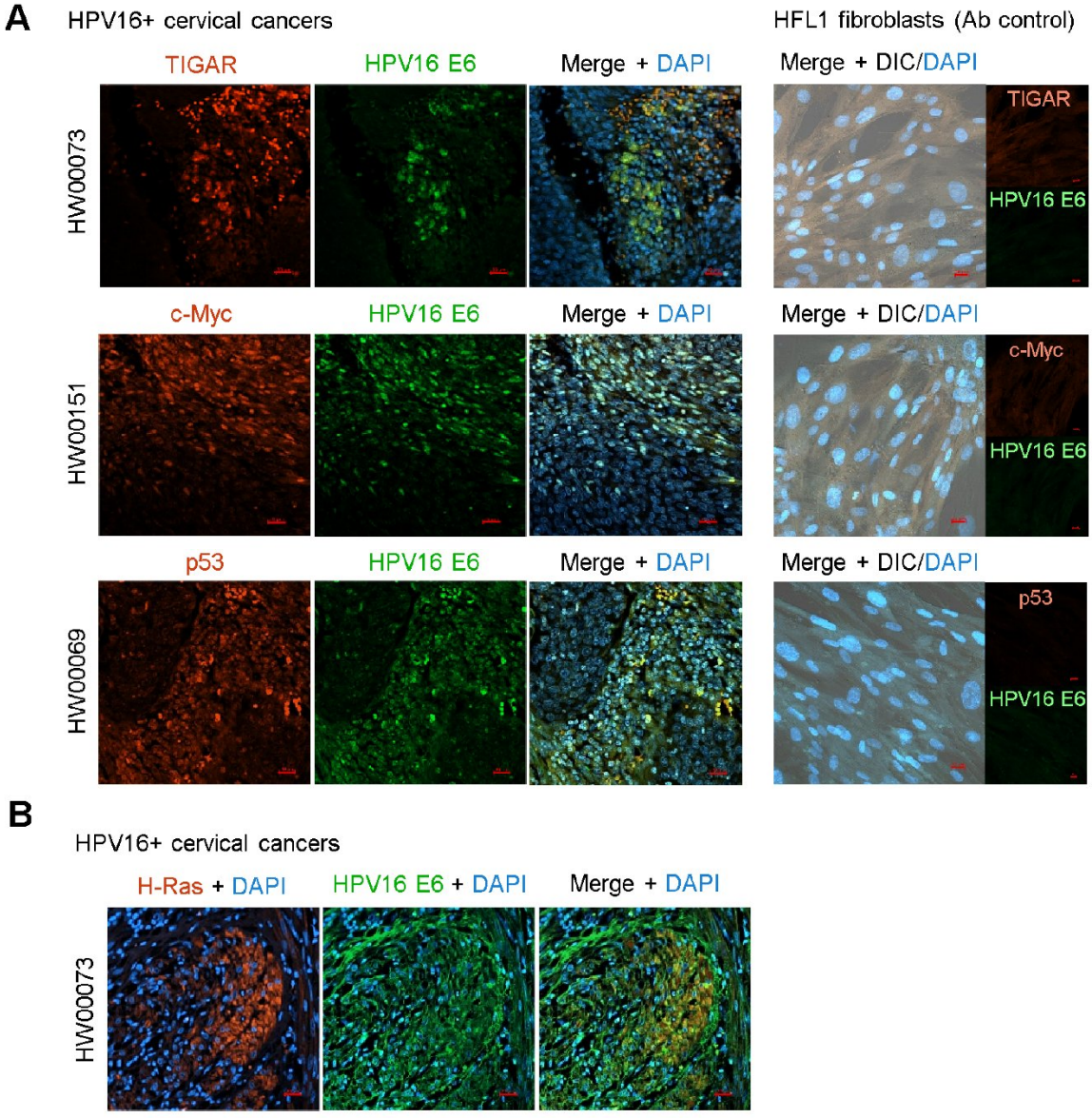

Supplemental Fig. S10. Primary HPV16+ cervical cancer clinical isolates contain detectable TIGAR, c-Myc, H-Ras, and p53 protein expression. (A) To determine how TIGAR, c-Myc, and p53 contribute to hrHPV-induced carcinogenesis, biopsied HPV16+ cervical carcinoma tissue samples (n-value = 9) were

kindly provided by the Pathology Shared Resource of the University of Hawaii Cancer Center and analyzed by immunofluorescence-confocal microscopy to quantify the relative percentages of HPV16 E6-positive cells (green signal) that contain TIGAR, c-Myc, or p53 protein expression (red signal) as shown in Fig. 6G. DAPI nuclear-staining (blue signal) and DIC phase-contrast are provided in the merged images. Human HFL1 fibroblasts were immunostained as an HPV-negative antibody (Ab) control (right panels). (B) The expression of H-Ras (red signal) was visualized within the HPV16 E6-positive tumor cells using immunofluorescence-confocal microscopy. Scale bar, 20 μm. The data in A and B is representative of triplicate fields for each tissue section.

Supplemental Table S1. Antibodies, Chemicals and reagents, Cell-lines, Clinical samples, Animal strains, Lentiviruses, and DNA plasmids.

Antibodies

Antibody ID	Source	Cat. number
Rabbit polyclonal Anti-TIGAR (M-209)	Santa Cruz Biotechnology	sc-67273
Rabbit polyclonal Anti-TIGAR (ab2)	Millipore-Sigma	PRS4051-100UG
Mouse monoclonal Anti-TIGAR (F-5)	Santa Cruz Biotechnology	sc-377065
Mouse monoclonal Anti-c-Myc (9E10)	Santa Cruz Biotechnology	sc-40
Mouse monoclonal Anti-c-Myc (9E10)	Millipore-Sigma	M5546-100UL
Mouse monoclonal Anti-p53 (DO-2)	Santa Cruz Biotechnology	sc-53394
Mouse monoclonal Anti-HPV18E6 + HPV16 E6 (C1P5)	Abcam	ab70
Goat polyclonal Anti-HPV16 E6 (N-17)	Santa Cruz Biotechnology	sc-1584
Rabbit polyclonal Anti-HA probe (Y-11)	Santa Cruz Biotechnology	sc-805
Rabbit polyclonal Anti-Beta Actin	Abcam	ab8227
Mouse monoclonal Anti-HA probe (HA.C5)	Santa Cruz Biotechnology	sc-57595
Goat polyclonal Anti-HPV18 E6 (N-17)	Santa Cruz Biotechnology	sc-1586
Mouse monoclonal Anti-FLAG M2	Millipore-Sigma	F1804-200UG
Mouse monoclonal Anti-Phospho-threonine	Millipore-Sigma	P6623-100UL
Mouse monoclonal Anti-Phospho-serine	Millipore-Sigma	P5747-100UL
Mouse monoclonal Anti-Phospho-tyrosine	Millipore-Sigma	P4110-1MG
Mouse monoclonal Anti-Alpha Tubulin (TU-02)	Santa Cruz Biotechnology	Sc-8035

Rabbit monoclonal Anti-TOMM20 (EPR15581-54)	Abcam	ab186735
Rabbit monoclonal Anti-IκB alpha (E130)	Abcam	ab32518
Rabbit polyclonal Anti-GTPase H-Ras	Abcam	ab97488
Rabbit polyclonal Anti-Phospho-γH2A.X (Ser 139)	Santa Cruz Biotechnology	sc-101696
Mouse monoclonal Anti-Acetyl-K120-p53 (10E5)	Abcam	ab78316
Rabbit polyclonal Anti-p53 (FL-393)	Santa Cruz Biotechnology	sc-6243
Mouse monoclonal Anti-HIF-1 alpha (28b)	Santa Cruz Biotechnology	sc-13515
Rabbit polyclonal Anti-HIF-2 alpha	Abcam	ab199
Rabbit polyclonal Anti-human-Ki67 (H-300)	Santa Cruz Biotechnology	sc-15402
Rabbit polyclonal Anti-c-Myc (C-19)	Santa Cruz Biotechnology	sc-788
Mouse monoclonal Anti-VEGF (C-1)	Santa Cruz Biotechnology	sc-7269
Alexa Fluor 488 AffiniPure Donkey Anti-Mouse IgG (H+L)	Jackson Immunoresearch Laboratories	715-545-150
Alexa Fluor 488 AffiniPure Donkey Anti-Rabbit IgG (H+L)	Jackson Immunoresearch Laboratories	711-545-152
Alex Fluor 488 AffiniPure Donkey Anti-Goat IgG (H+L)	Jackson Immunoresearch Laboratories	705-545-003
Rhodamine (TRITC) AffiniPure Donkey Anti-Mouse IgG (H+L)	Jackson Immunoresearch Laboratories	715-025-150
Rhodamine (TRITC) AffiniPure Donkey Anti-Goat IgG (H+L)	Jackson Immunoresearch Laboratories	705-025-003
Rhodamine (TRITC) AffiniPure Donkey Anti-Rabbit IgG (H+L)	Jackson Immunoresearch Laboratories	711-025-152
Peroxidase-conjugated AffiniPure Donkey Anti-Mouse IgG (H+L)	Jackson Immunoresearch Laboratories	715-035-150
Peroxidase-conjugated AffiniPure Goat Anti-Rabbit IgG (H+L)	Jackson Immunoresearch Laboratories	111-035-144
Peroxidase-conjugated AffiniPure Donkey Anti-Goat IgG (H+L)	Jackson Immunoresearch Laboratories	705-035-147

Chemicals and reagents

Chemical name	Source	Cat. number
Carbonyl cyanide 3-chlorophenylhydrazone (CCCP)	Millipore-Sigma	C2759
Wortmannin	Millipore-Sigma	W1628
Staurosporine	Millipore-Sigma	S5921
SB 203580	Millipore-Sigma	S8307
Ponceau S (anhydrous)	Millipore-Sigma	78376-10G-F
Recombinant serine/threonine-protein phosphatase	Abcam	ab188459

Cell-lines

Cell-line ID	Source	Cat. number
HeLa (HPV18+)	ATCC	CCL-2
MS751 (HPV18/HPV45+)	ATCC	HTB-34
C-4 I (HPV18+)	ATCC	CRL-1594
SiHa (HPV16+)	ATCC	HTB-35
Ca Ski (HPV16+)	ATCC	CRL-1550
HT-1080	ATCC	CCL-121
HFL1	ATCC	CCL-153
HEKn (Primary epidermal keratinocytes, human neonatal foreskin)	ATCC	PCS-200-010
HDFn (Primary dermal fibroblasts, human neonatal foreskin)	ATCC	PCS-201-010
HCT116 *p53*-null (CRISPR KO)	Horizon Discovery Biosciences	HD 104-001
293FT	Invitrogen	R70007
293 HEK	ATCC	CRL-1573

Primary HPV16+ cervical carcinoma clinical samples

Sample ID	Source	IRB protocol #
HW00069	University of Hawaii Cancer Center	2016-019-Harr
HW00073	University of Hawaii Cancer Center	2016-019-Harr
HW00104	University of Hawaii Cancer Center	2016-019-Harr
HW00107	University of Hawaii Cancer Center	2016-019-Harr
HW00116	University of Hawaii Cancer Center	2016-019-Harr
HW00151	University of Hawaii Cancer Center	2016-019-Harr
HW00185	University of Hawaii Cancer Center	2016-019-Harr

HW00189	University of Hawaii Cancer Center	2016-019-Harr
HW00206	University of Hawaii Cancer Center	2016-019-Harr

Animal strains

Genus/species/strain	Source	Cat. Number
Mus musculus, NIH-III nude	Charles River Laboratories	NIH-III nude mouse

Lentiviruses

Virus ID	Source	Cat. number
pLenti-siRNA-*tigar*	Robert Harrod Lab	N/A
pLenti6.2/V5-DEST vector	Invitrogen	V36820

DNA plasmids

Plasmid ID	Source	Cat. Number
pLenti-siRNA-*tigar* construct	Robert Harrod Lab	N/A
pLenti6.2/V5-DEST plasmid	Invitrogen	V36820
GATEWAY pCR8/GW/TOPO entry vector cloning kit	Invitrogen	K250020
ViraPower Lentiviral Packaging Mix (pLP1, pLP2, and pLP/VSVG plasmids)	Invitrogen	K497500
GWI-HPV18 E6 (HA-tagged)	Lawrence Banks Lab	N/A
pcDNA3-HPV16 E6 (HA-tagged)	Lawrence Banks Lab	N/A
pCEP-wild-type-p53	Bert Vogelstein Lab	N/A
pCEP-p53-R175H mutant	Bert Vogelstein Lab	N/A
pOZ-TIP60 (HA-tagged)	Yoshihiro Nakatani Lab	N/A
N3-pEGFP	Clontech	N/A
pcDNA3.1-TIGAR (FLAG-tagged)	Karen Vousden Lab	N/A
pLNCX2-PI5P4Kβ (FLAG-tagged)	Lewis Cantley Lab	N/A
pLNCX2 vector	Lewis Cantley Lab	N/A
pUSEamp-PI3-K p110α (HA)	Upstate Biotechnology	21-160
pcDNA-AKT (HA-tagged)	Chou-Zen Giam Lab	N/A
CβF-c-Myc (FLAG-tagged)	Michael Cole Lab	N/A
CβS vector	Michael Cole Lab	N/A